Science Advances
AAAS

advances.sciencemag.org/cgi/content/full/6/24/eaba4171/DC1

Supplementary Materials for

Mapping the 3D orientation of nanocrystals and nanostructures in human bone: Indications of novel structural features

Tilman A. Grünewald, Marianne Liebi, Nina K. Wittig, Andreas Johannes, Tanja Sikjaer, Lars Rejnmark, Zirui Gao, Martin Rosenthal, Manuel Guizar-Sicairos, Henrik Birkedal*, Manfred Burghammer*

*Corresponding author. Email: hbirkedal@chem.au.dk (H.B.); manfred.burghammer@esrf.fr (M.B.)

Published 12 June 2020, *Sci. Adv.* **6**, eaba4171 (2020)
DOI: 10.1126/sciadv.aba4171

The PDF file includes:

Other Supplementary Material for this manuscript includes the following:

(available at advances.sciencemag.org/cgi/content/full/6/24/eaba4171/DC1)

Supplementary Information

Movie S1. Slice through the tomograms of the reconstructed SAXS, WAXS and orientation difference (left, middle, right). Color code is degree of orientation for SAXS and WAXS, the orientation difference is shown by the color code (squared dot product, value 1 corresponds to perfect co-alignment).

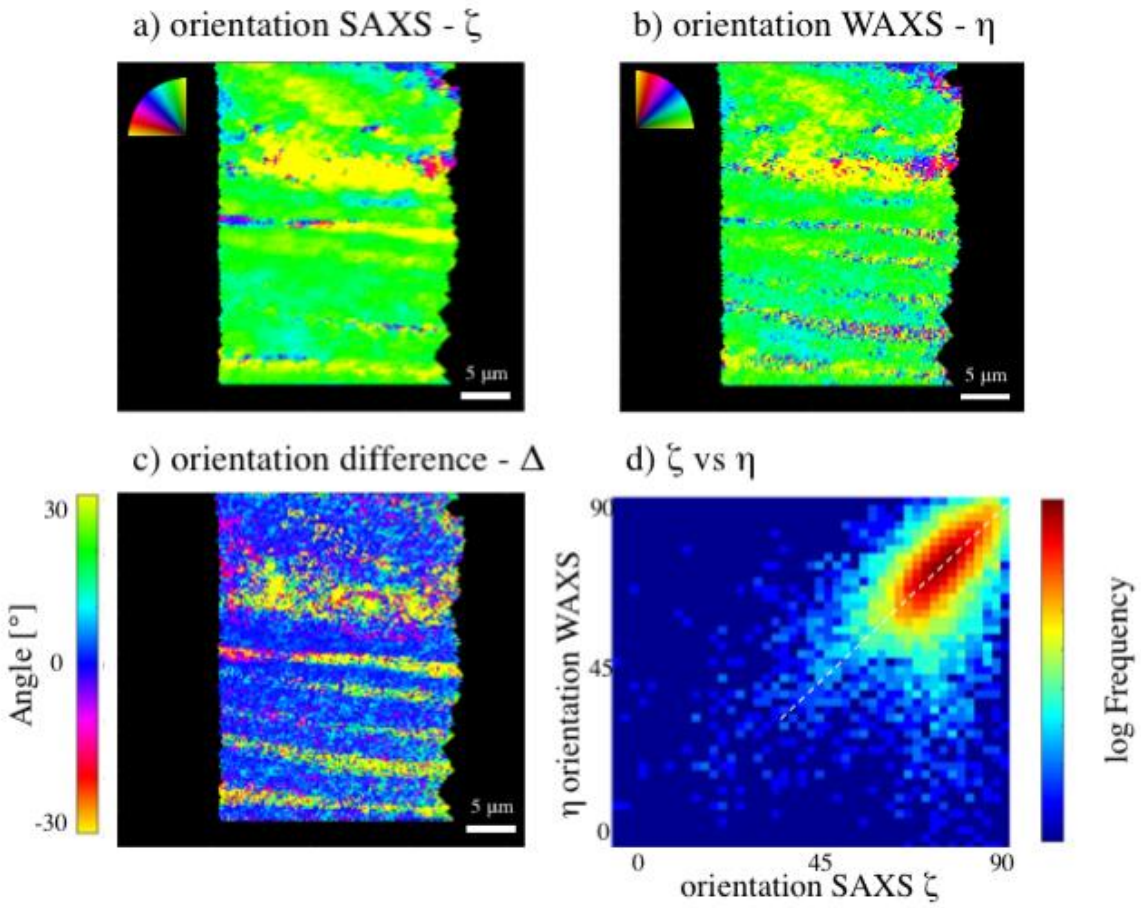

Fig. S1. 2D scan of a 3 µm section of healthy bone. Scanning diffraction of a FIB-thinned slice of human osteonal bone and the orientation of the nanostructure ζ (from SAXS) (a), the crystallographic c-axis η (from WAXS) (b) and their orientation difference Δ=90°+ζ-η (c). The 2D histogram (d) of the alignment ζ vs. η-90°. The major fraction of SAXS/WAXS is clearly co-aligned with a significant portion of orientation difference.

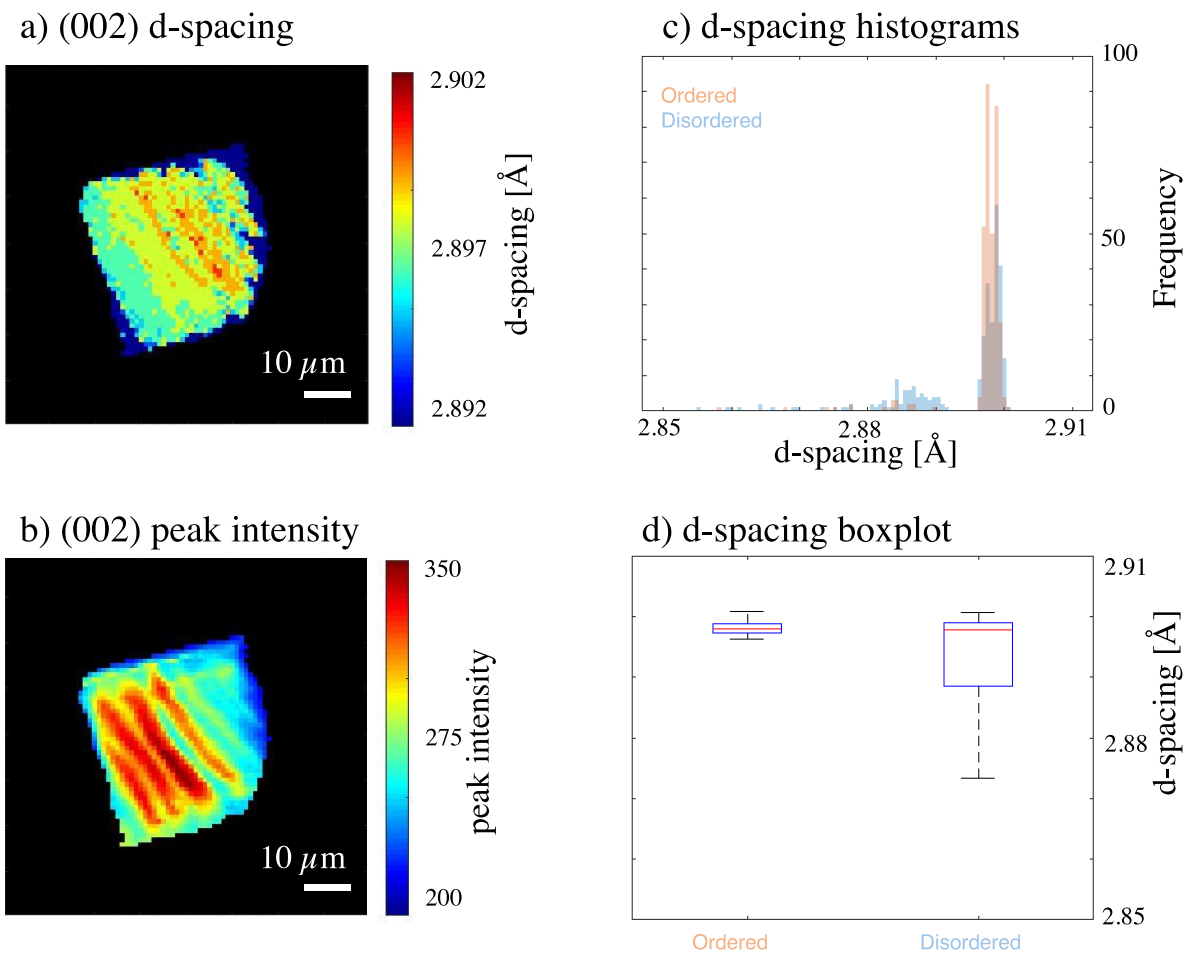

Fig. S2. (002) *d*-spacing, intensity and distribution within the bone cube. a) The d-spacing shows a shift towards smaller lattice constants in the differently oriented zones. b) The (002) intensity shows the banding of co-oriented and differently oriented zones in the sample. c) Histogram of the d-spacing in ordered (red) and disordered (blue) shows the shift towards smaller d-spacing. d) Boxplot of the two ordered and disordered fractions shows the broadening of the box in the case of disordered zones.

<u>Alternative reconstruction of the orientation tensor (IRTT)</u>

In order to test the starting guess of rotational invariance around the respective fiber axes for SAXS and WAXS data, we reconstructed the data with a recently published alternative reconstruction approach (*33)* that models the scattering signal with a rank-2 tensor. For the problem at hand, it describes the orientation tensor as an ellipsoid, effectively allowing for an intensity variation around the fiber axis. From this, a fiber index If can be calculated as:

$$If = \frac{e1-e2}{0.5(e1+e2)}$$

for each voxel, with *e1* and *e2* being the 1st and 2nd eigenvalues of the tensor, which represent the distribution of intensity value distribution perpendicular to the fiber axis.

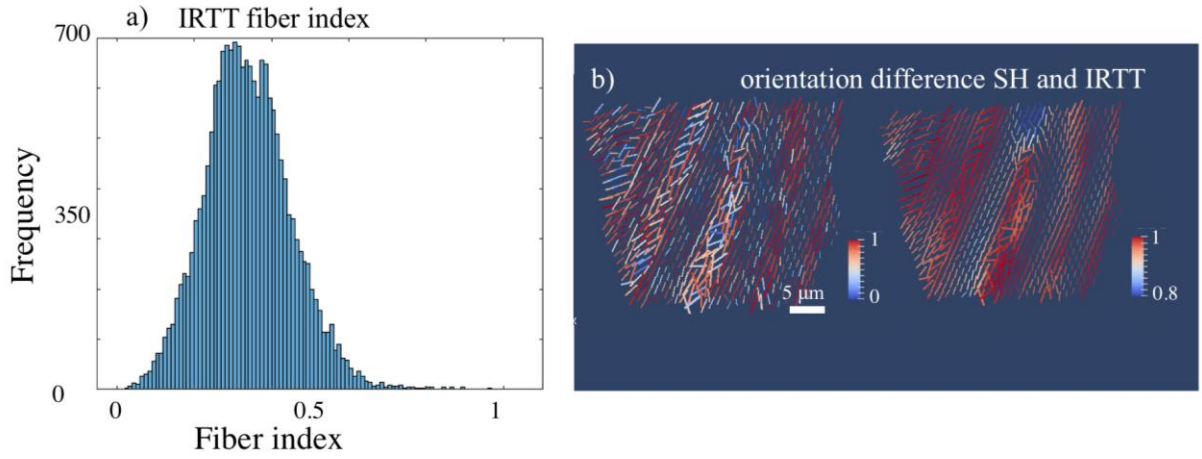

Fig. S3. IRTT reconstructions and comparison to spherical harmonics reconstructions. a) Histogram of the fiber index of the whole volume. A center of the distribution at around 0.34 can be observed with a normal distribution of fiber indices. b) Comparison of the SAXS/WAXS orientation difference reconstructed by SH and IRTT. It is evident that the same banded localization is visible in both SH and IRTT reconstructions. Due to the different reconstruction algorithms, the magnitudes differ between the two; the localization of the orientation difference however stays fixed.

Figure S3 shows a histogram of ratio, with an average value around 0.34, meaning that the two half-axes show about 30% deviation from a perfect fiber texture with two equal axes. It is however noteworthy, that the histograms of co-oriented and differently oriented fractions exhibit a very similar mean and variance and we thus conclude that the deviation rather stems from noise in the reconstruction. By applying the IRTT reconstruction to the WAXS data as well, we were able to compare the orientations of the two components in a similar fashion. Figure S2b shows the squared dot product of the two main orientations in a slice through the sample similar to Fig 2e. It is evident, that the same localization of misorientation can be seen, albeit on a slightly less pronounced level. This is most probably due to the fact that the WAXS IRTT reconstructions do not account in the current implementation for the curvature of the Ewald sphere as well as the tendency of the IRTT reconstructions to allocate intensity in a continuous fashion over adjacent voxels, effectively smoothing the local structure slightly.